Copper Ions Inhibit *S*-Adenosylhomocysteine Hydrolase by Causing Dissociation of NAD^+ Cofactor†

Mengyao Li,‡ Yanjie Li,‡ Jiejin Chen,‡ Wei Wei, Xiaowei Pan, Jing Liu, Qingyu Liu, Wei Leu, Liangren Zhang, Xiaoda Yang,* Jingfen Lu, and Kui Wang

Department of Chemical Biology and State Key Laboratories of Natural and Biomimetic Drugs, School of Pharmaceutical Sciences, Peking University Health Science Center, Beijing 100083, People's Republic of China

Received February 27, 2007; Revised Manuscript Received August 9, 2007

ABSTRACT: *S*-Adenosylhomocysteine hydrolase (SAHH) regulates biomethylation and homocysteine metabolism and thus is an attractive target in drug design studies. SAHH has been shown to be a copper binding protein in vivo; however, the structure and catalytic mechanism of SAHH exclude a role for Cu^{2+}. In the present work, we studied the mechanism of inhibition of SAHH activity by Cu^{2+}. The experimental results showed that Cu^{2+} inhibited SAHH activity in a noncompetitive manner. Binding of Cu^{2+} to SAHH resulted in the release of NAD^+ cofactors, explaining the loss of the enzymatic activity of SAHH. Further investigation by an ESR probe and computational simulation suggested that Cu^{2+} could bind at the central channel and interrupt the subunit interactions of SAHH, resulting in a large decrease in affinity to the NAD^+ cofactor. This effect of Cu^{2+} resembled that of enzyme mutations at the C-terminal domain or Asp244 [Komoto, J., Huang, Y., Gomi, T., Ogawa, H., Takata, Y., Fujioka, M., and Takusagawa, F. (2000) Effects of site-directed mutagenesis on structure and function of recombinant rat liver S-adenosylhomocysteine hydrolase. Crystal structure of D244E mutant enzyme, *J. Biol. Chem. 275*, 32147−32156]. The mechanism of action of Cu^{2+} on SAHH suggested a possible regulative role for Cu^{2+} on the intracellular activity of SAHH. This could be helpful in understanding the biological effects of copper compounds and suggest a potential coupling mechanism between biomethylation and the redox states of cells.

S-Adenosylhomocysteine (AdoHcy)[1] is the product of all adenosylmethionine (AdoMet)-dependent biological transmethylations and acts as a potent inhibitor of AdoMet-dependent methyltransferases. By controlling the levels of AdoHcy, SAHH plays a vital role in the regulation of biomethylation in proliferating cells (*2*). In addition, an elevated level of plasma Hcy (hyperhomocysteinemia, hyperHcymia) has been suggested to be an independent risk factor for cardiovascular disease (*3*) and closely associated with diabetes (*4*), cancer (*5*), and a variety of degenerative diseases, e.g., Alzheimer's disease (*6*, *7*). Hydrolysis of AdoHcy promoted by *S*-adenosylhomocysteine hydrolase (SAHH) in eukaryotic cells produces adenosine (Ado) and homocysteine (Hcy) (*8*, *9*). Ado has been suggested to be very important in renal (*10*), cardiovascular (*11*), and neuronal (*12*) functions. SAHH has been used as the target for designing antiviral, antiparasitic, antiarthritic, immunosuppressive, and antitumor drugs (*8*, *13*).

The structures and catalytic mechanism of SAHH have been elucidated (*9*, *14*−*22*). Although the structure and catalysis of SAHH did not involve any copper ions, SAHH was shown to be a copper binding protein in vivo, and its expression level was sensitive to the copper status in animals (*23*, *24*). Some in vivo studies have suggested a close relationship between the activity of SAHH and the copper level; e.g., hyperHcymia was found to associate with an increased serum copper level (*25*). Copper ions could increase the intracellular release of homocysteine (*26*), an effect similar to that of some inhibitors of SAHH (*9*).

It was suggested that SAHH may play an important role in copper metabolism (*27*), but the role of copper ions in SAHH activity has not been clarified. Nonetheless, elucidating the mechanisms of copper ions on the activity and structure of SAHH would be helpful for understanding the apparently contradictory roles of copper and SAHH. Previously, we demonstrated that copper ions bind to SAHH with a real K_d of $\sim 10^{-12}$, thus inactivating the enzyme (*28*, *29*). As speculated previously (*15*), some potential metal ion binding sites were located in the central channel of the tetrameric enzyme. The unique channel structure would provide a strong core framework and offer mobility to the catalytic domains (*15*).

† This work is supported by the National Natural Science Foundation of China (Grant 20331020) and 985 program.

* To whom correspondence should be addressed. Phone: +86-010-8280-1539. Fax: +86-010-6201-5584. E-mail: xyang@bjmu.edu.cn.

‡ These authors contributed equally to the current study.

[1] Abbreviations: SAHH, *S*-adenosylhomocysteine hydrolase; Ado, adenosine; AdoHcy, *S*-adenosylhomocysteine; Hcy, homocysteine; AdoMet, adenosylmethionine; DNTB, 5,5′-dithiobis(2-nitrobenzoic acid); MOPS, 3-(*N*-morpholino)propanesulfonic acid; DHCeA, 2′,3′-dihydroxycyclopent-4-enyladenine; HPLC, high-performance liquid chromatography; ESR, electron spin resonance; MALDI-TOF MS, matrix-assisted laser desorption ionization time-of-flight mass spectrometry.

10.1021/bi700395d CCC: $37.00
Published on Web 09/25/2007

In the present work, we describe the mechanism by which Cu^{2+} inhibited the activity of SAHH. Cu^{2+} may bind to the central channel of SAHH and interrupt subunit cooperation of the enzyme, thus causing release of the cofactor NAD^+. Defining the interaction of copper with SAHH would be helpful in understanding the biological effects of copper compounds and a possible coupling mechanism between biomethylation and the redox states of cells.

EXPERIMENTAL PROCEDURES

Materials. Escherichia coli JM109 strain transformed with a plasmid (pPROK-1) encoding human placental SAHH was obtained from the University of Kansas. Adenosine (Ado), homocysteine (Hcy), adenosylhomocysteine (AdoHcy), 5,5′-dithiobis(2-nitrobenzoic acid) (DTNB), NAD^+, NADH, 3-(*N*-morpholino)propanesulfonic acid (MOPS), 2′,3′-dihydroxycyclopent-4-enyladenine (DHCeA), trypsin, and maleimide were purchased from Sigma Co. (Missouri). All other chemicals were analytical reagent grade.

Enzyme Preparation and Reconstitution. The native-form SAHH was expressed in JM109 and purified using the procedures described by Yuan et al. (*30*). The enzyme purity was checked using SDS−polyacrylamide gel electrophoresis (PAGE), and the protein concentration was determined by the Bradford method (*31*) using bovine serum albumin as a standard.

The apo-form enzyme was prepared by precipitating the enzyme with an acidic ammonium sulfate solution as described by Porter (*18*) and Yuan et al. (*30*) previously. The NAD^+ (or NADH)-form enzyme was prepared by incubation of the apoenzyme with an excessive amount of NAD^+ (or NADH) by Porter (*18*) and Gomi et al. (*32*). The unbound cofactors were removed using a PD-10 Sephadex G-25 desalting column (Amersham Pharmacia Biotech) equilibrated by a buffer containing 0.050 M potassium phosphate and 1 mM EDTA, pH 7.2, according to the procedure provided by the manufacturer.

The enzyme buffer was changed to a MOPS reaction buffer (20 mmol/L MOPS, pH 7.4) before incubation with copper ions by passing the solution through a PD-10 desalting column equilibrated with the MOPS reaction buffer.

Assays for Enzyme Activities. The assay of SAHH activity in the synthetic direction was performed as decribed by Yuan et al. (*30*) by measuring the rate of formation of AdoHcy from Ado and Hcy using an HPLC system (Hitachi, L-2400). The assay of SAHH activity in the hydrolytic direction used the spectrophotometric method decribed by Yuan et al. (*30*) by measuring the rate of the product Hcy formed by reaction with DTNB.

Inhibition Assays. In a total volume of 250 μL in MOPS reaction buffer, 2 μg of SAHH was incubated with a range of concentrations of copper ion ($CuSO_4$) at 37 °C for 30 min. The incubation time of 30 min was chosen on the basis of our preliminary studies of the time-dependent process of copper ion inhibition (*28*). Then 250 μL of substrate solution containing 0.5−100 μM Ado and 5 mM Hcy (or 500 μM Ado and 0.01−4.0 mM Hcy) was added. After incubation at 37 °C for 5 min, the remaining activity of SAHH was measured in the synthetic direction using HPLC as described above.

For inhibition assays in the presence of substrate AdoHcy, 1 μg of SAHH was mixed with a range of copper ion concentrations in a total volume of 150 μL in MOPS reaction buffer and incubated at 37 °C for 30 min. Then 50 μL of solution containing various concentrations of AdoHcy, 400 μM DTNB, and 1 unit of Ado deaminase was added. Then the remaining activity of SAHH was measured in the hydrolytic direction as described above.

The kinetic parameters of enzyme inhibition by copper ions were obtained through a double-reciprocal plot ($1/v \approx 1/[S]$) using a Micro Origin program (Originlab Co., Northampton, MA). The inhibition constant K_i was calculated using the Origin program by data fitting to the following equation:

$$V_{max}(\text{apparent}) = \frac{V_{max}}{1 + [Cu^{2+}]/K_i}$$

Effect of Copper Ions on Release and Reduction of the NAD^+ Cofactor. In a total volume of 1000 μL of MOPS reaction buffer, 0.24 mg/mL NAD^+-form SAHH was incubated with various concentrations of copper ions at 37 °C for 30 min. Then 500 μL of the reaction mixture was transferred to a Millipore Ultrafree-4 centrifugal filter (MW 30K cutoff) and centrifuged at 2000*g* for 15 min. The filtrate (200 μL) was then assayed for NAD^+/NADH content using the fluorescence methods described previously (*33*). Briefly, NADH was determined directly by excitation at 340 nm and measurement of emission at 460 nm, and NAD^+ was measured after its conversion to NADH by adding 10 μL of a 1% solution of baker's yeast alcohol dehydrogenase and 20 μL of 97% ethanol.

Meanwhile, 10 μL of 5 mM 2′,3′-dihydroxycyclopent-4-enyladenine (DHCeA) was added to the other 500 μL reaction mixture and the resulting mixture incubated at 37 °C for a further 30 min. Then the samples were assayed for NAD^+/NADH content by the fluorescence methods as described (*33*).

Effect of Copper Ions on NAD^+ Binding. To 250 μL of MOPS reaction buffer containing various concentrations of NAD^+ and 0, 60, and 120 nmol/L copper ions was added 1 μg of apo-form SAHH, and the samples were incubated at 37 °C for 3 h. Our preliminary studies showed that the apoenzyme recovered activity in 1−2 h upon incubation with NAD^+ and the SAHH activity remained unchanged for at least 24 h at 37 °C. Then the activity of SAHH was measured in the synthetic direction after the addition of 50 μL of 10 mM Ado and 200 μL of 10 mM Hcy described above. The dissociation constant of NAD^+ to SAHH was obtained by plotting the enzyme activity versus NAD^+ cofactor concentrations and fitting the data to a Hill equation using an Origin program.

Preparation of Spin-Labeled SAHH (SAHH−MSL). Specific labeling of the cysteine 421 residue with 3-maleimide-2,2,5,5-tetramethyl-1-pyrrolidinyloxyl (MSL) was carried out in the presence of Ado as described previously (*30*, *34*). Briefly, 10 mg of SAHH was dissolved in 3.0 mL of pH 8.0 PBS buffer and the resulting solution mixed with 2.4 mL of 5 mM Ado. After the sample was preincubated at room temperature for 10 min, 250 μL of 1 mM MSL was added. The mixture was kept in the ice−water bath for 3 min and then left at 4 °C in darkness for 10 h to complete the reaction. Then the substrate Ado and the excessive amounts of MSL

were removed by five washes at 4 °C in the dark using a centrifugal ultrafiltration tube (Millipore, size 30 kDa) according to the protocol provided by the manufacturer.

Electron Spin Resonance (ESR) Measurements. Samples of Cu−SAHH complexes (1:1 and 1:2 enzyme subunit to copper ion ratio) and Cu−SAHH−MSL complexes with a 1:1 molar ratio of the enzyme subunit to copper ions were both prepared by incubation of SAHH or SAHH−MSL with copper ions in MOPS reaction buffer. For measurement of the ESR signal of Cu−SAHH−MSL complexes, the unbound copper ions were removed using a centrifugal ultrafiltration tube (Millipore, size 30 kDa) according to the manufacturer's protocol. The protein samples (SAHH, Cu−SAHH complexes, SAHH−MSL, Cu−SAHH−MSL complexes) were lyophilized and dissolved in PBS. Then the ESR spectra of the samples were scanned on a Bruker ESR 300 spectrometer with a rectangular TE102 at 77 K at the X-band.

The measurement conditions were microwave frequency 9.433 GHz (X-band), microwave power 20 mW, central magnetic field 3360 G, sweep width 100 G, sweep time 60 s, TC = 163 ms, modulation frequency 100 kHz, modulation amplitude 5.1 G, and room temperature. All final data have been reported as the mean of replicates (±SD).

Calculation of the distance from copper ions to the spin label MSL was carried out on the basis of the theory of the dipolar interaction between two different electron spins bound to the same macromolecule (*35*). The line width (δH) of the observed ESR signal of the nitroxyl radical could be given by the following equation:

$$\delta H = \frac{2\pi g\beta\mu^2\tau}{r^6 h}(1 - 3\cos^2\theta'_R)^2 + \delta H_0 \qquad (1)$$

where g and β are the g factor and bohr magneton, respectively, h refers to the Planck constant, μ is the magnetic moment constant, τ is the electron spin relaxation time, r is the distance between the copper ion and the nitroxyl free radical, θ_R' is the angle between the dipole position vector and the magnetic field direction, and δH_0 is the natural line width in the absence of dipolar broadening.

The values of δH and δH_0 were obtained from the relative amplitudes of the ESR signals of the spin label−enzyme complex in the presence and absence of copper ions. The values of τ were estimated according to the equation

$$\tau = (6.51 \times 10^{-10})(\delta H_0)[(h_0/h_{-1})^{0.5} + (h_0/h_{+1})^{0.5} - 2] \qquad (2)$$

The values of h_0, h_{-1}, and h_{+1} correspond to the heights of the middle-field, high-field, and low-field lines of the spectra of the MSL−enzyme complex in the presence of copper ions, respectively.

Computational Search for Copper Binding Sites. Computational manipulation of the SAHH structure was based on the crystal structure of SAHH (PDB code 1A7A). MSL was added to Cys421 using the Bioplomer module of the InsightII program (Accelrys Co.). The energy of the structure was minimized by 300 steps in a combination of steepest descent and conjugated gradient using Discover 3 (Accelrys Co.) while the structure of SAHH was held fixed. The hydrogen acceptor sites, which were assigned to be copper binding sites, were searched from Cys421 within 20 Å (the distance from the N−O• free radical of MSL to the copper site plus the distance from Cys421 to the free radical) using the Ludi module of the Insight II program.

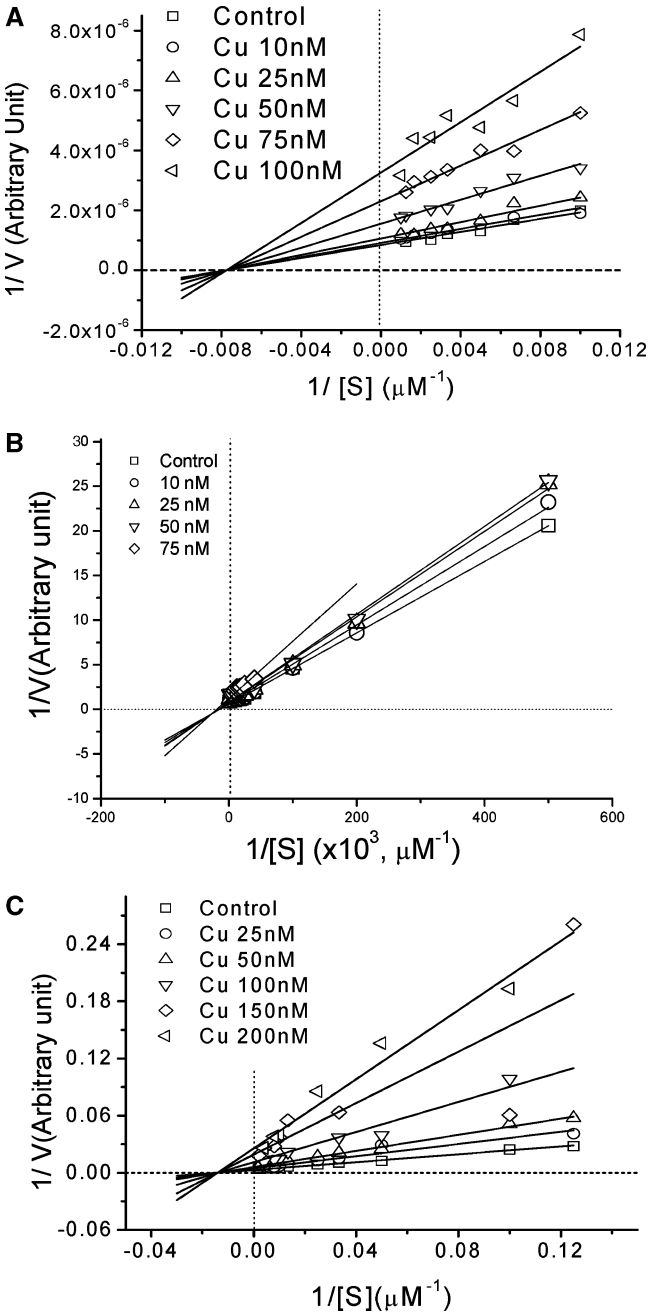

FIGURE 1: Double-reciprocal plot of SAHH activity and substrate concentrations in the presence of various concentrations of Cu^{2+}. (A)−(C) refer to substrates Hcy ([Ado] = 500 μM), Ado ([Hcy] = 5.0 mM), and AdoHcy, respectively. SAHH (~2 μg/500 μL) was incubated with a variety of concentrations of copper ions at 37 °C for 30 min. Then the desired concentrations of substrates were added, and the activity of SAHH was measured in the synthetic or hydrolytic direction as described previously (*29*, *30*) by measuring the rate of formation of AdoHcy from Ado and Hcy using an HPLC system or the rate of the product Hcy formed by reaction with DTNB. See the text for details.

RESULTS

Inhibition Kinetics. Figure 1shows double-reciprocal plots of SAHH in the presence of various concentrations of Cu^{2+}. The correlation coefficients (r^2) of the data fitting above were

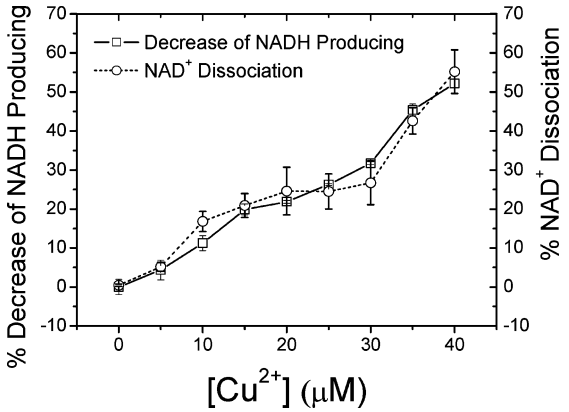

FIGURE 2: Effects of Cu^{2+} on NAD^+ dissociation and NADH production of SAHH. A 0.24 mg/mL concentration of NAD^+-form SAHH was incubated with various concentrations of copper ions at 37 °C for 30 min. Then the reaction mixture was applied to a Millipore Ultrafree-4 centrifugal filter (MW 30K cutoff), and the filtrate was assayed for NAD^+/NADH content using the fluorescent methods as described previously (*33*). See the text for details.

between 0.972 and 0.996. For all three substrates Ado, Hcy, and AdoHcy, V_{max} decreased with an increase of Cu^{2+}, while K_M basically was constant, suggesting a pattern of noncompetitive inhibition (a special case of mixed inhibition). For all the substrates, identical inhibition constants were obtained, 25 ± 5 nM, which is very close to our previous determination (14 ± 5 nM) (*28*).

Effects of Copper Ions on Binding of Cofactors to SAHH. The results in Figure 2 indicate that incubation of SAHH with Cu^{2+} resulted in dissociation of NAD^+ from SAHH in a concentration-dependent manner. Meanwhile, Cu^{2+} decreased the formation of NADH upon incubation of SAHH with DHCeA, which is a type I inhibitor of SAHH and could result in complete reduction of NAD^+ to NADH. The percentage of NADH decrease in the substrate-bound NADH form was essentially equal to the percentage of NAD^+ dissociation from SAHH with an increase of the concentration of Cu^{2+}; however, release of the NADH cofactor from the substrate-bound NADH-form enzyme was not observed in the experiments.

The binding affinity of NAD^+ to the apo-form enzyme was determined as described previously, and the results are shown in Figure 3. The K_d of NAD^+ to SAHH was calculated to be 153 ± 23 nM, which is close to that previously reported (*36*, *37*); however, the K_d value increased to 150 ± 46 μM and 1.0 ± 0.2 mM in the presence of 60 and 120 nM Cu^{2+}, respectively. The pattern of the double-reciprocal plot (Figure 3B) ($r^2 = 0.974$) with the straight lines intersecting y intercepts indicated an apparent competitive inhibition pattern.

ESR Analysis. There was one specific and high-affinity Cu^{2+} site for each subunit of SAHH (*38*); however, the Cu−SAHH (1:1) complexes were found to exhibit a very weak ESR signal (Figure 4, curve 1). Compared with the ESR signal of nonspecific Cu^{2+} (the 2:1 Cu−SAHH complexes; Figure 4, curve 2), the ESR signal of the specific Cu^{2+} was reduced by at least 15-fold. This result indicated that the specific Cu^{2+} binding sites on SAHH must be very close to each other so that their ESR signals would be quenched due to spin−spin interaction.

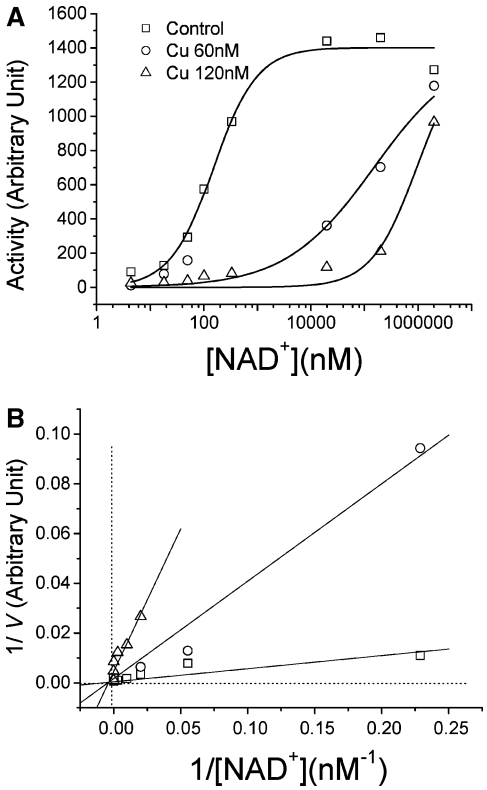

FIGURE 3: Untransformed (A) and double-reciprocal plot (B) of SAHH activity and NAD^+ concentrations in the presence of 0, 60, and 120 nM copper ions. The apo-form SAHH (~2 μg/500 μL) was incubated with various concentrations of NAD^+ in the absence/presence of copper ions at 37 °C for 3 h. The activity of SAHH was measured in the synthetic direction as described previously (*33*). See the text for details.

To locate the Cu^{2+} binding sites, the enzyme was labeled with a spin probe at Cys421 by incubation in the presence of substrate Ado. The labeled enzyme was tested for enzyme activity in the hydrolytic direction and was found to be the same as that of the native enzyme, which is consistent with the literature in that Cys421 is not crucial for the enzyme activity (*30*) and chemical modification of Cys421 will not affect the SAHH activity (*8*, *30*). As shown in Figure 5, upon binding of Cu^{2+}, the signal of MSL decreased 70% in amplitude. It had been proposed by Taylor et al. (*39*) that the decrease in the amplitude of the ESR spectrum of the spin-labeled enzyme was due to its interaction with paramagnetic ions within the specifically limited distance. On the basis of this interaction theory, the distance of the paramagnetic Cu^{2+} and the N−O• free radical of the spin label MSL bound to Cys421 was calculated to be 8.6 ± 0.5 Å.

Computational Prediction of Copper Binding Sites. Within 9 Å from the spin label (i.e., 20 Å distance from Cys421), two sites were identified as rich in hydrogen acceptors (Figure 6). Site A was surrounded by Glu243, Asp245, and Asn248 in chain A and Lys426, His429, and Tyr430 in chain B; site B was formed by Thr261, Asp263, Arg285, and His286 in chain A and Thr407 and Gln413 in chain B. Site A was located inside the central channel structure of SAHH, while site B was in the surface of SAHH. The distances between the centers of sites A and B within one dimer were measured to be approximately 10 and 40 Å, respectively.

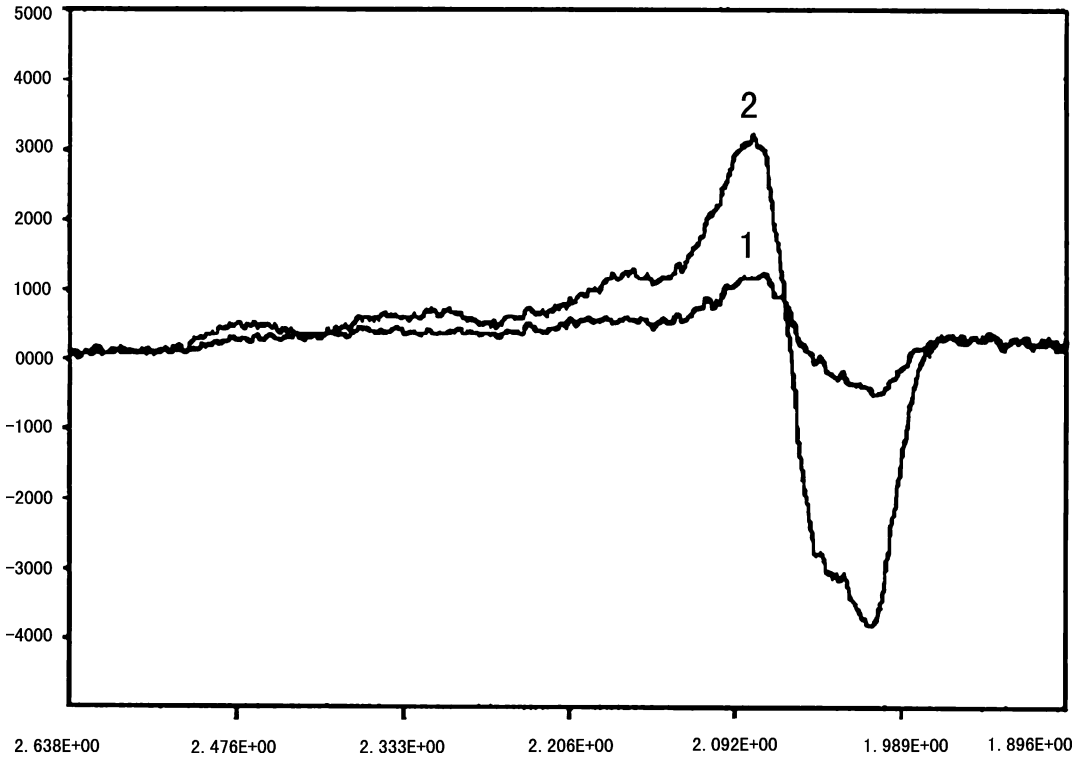

FIGURE 4: ESR spectra of Cu^{2+}−SAHH complexes: curve 1, 1 mM 1:1 Cu−SAHH complex; curve 2, 250 μM 2:1 Cu−SAHH complex. ESR spectra were recorded at 77 K at the X-band. See the text for details.

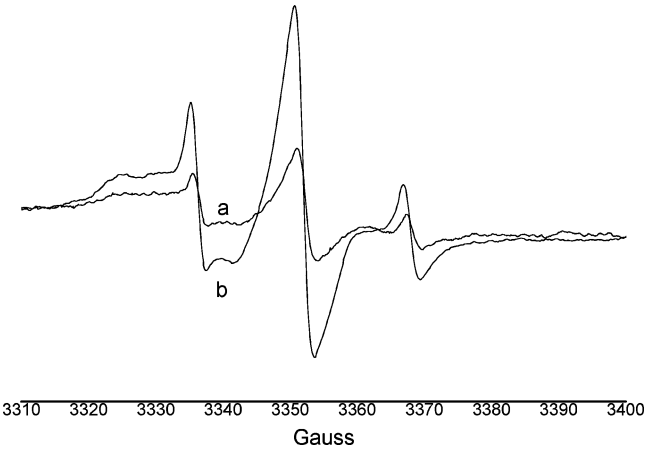

FIGURE 5: ESR spectra of enzyme-bound MSL spin label in the presence (a) and absence (b) of copper ions. The sample of Cu−SAHH−MSL was prepared by incubation of SAHH−MSL with equal moles of copper ions in MOPS reaction buffer. The unbound copper ions were removed by means of centrifugal ultrafiltration. The ESR spectra were recorded at $T = 77$ K and microwave frequency 9.433 GHz. See the text for details.

DISCUSSION

Mechanism by Which Cu^{2+} Inhibits SAHH. As proposed by several authors (*9*, *14*), SAHH has both partial redox and partial hydrolytic activities. The partial redox activity is conducted by an enzyme-bound NAD^+ cofactor. The mechanism-based inhibitors either trap the enzyme in the inactive NADH form (type I) or chemically modify the active site of the enzyme (type II) (*9*). We have previously shown (*28*, *29*) that Cu^{2+} bound to SAHH with a K_d of $\sim 10^{-12}$ M and inhibited the activity of SAHH in a concentration- and time-dependent manner. The present study further suggested that Cu^{2+} ions inhibit SAHH activity by causing dissociation of NAD^+ factors (Scheme 1). The supporting evidence included the following.

(1) The inhibition kinetics (Figure 1) revealed that Cu^{2+} inhibited SAHH activity in an apparent noncompetitive inhibition mode. These results suggested that Cu^{2+} could bind to free or substrate-bound enzyme but Cu^{2+} ions did not bind at the same site as the substrates.

(2) The apparent competitive inhibition pattern of NAD^+ (Figure 3) suggested that Cu^{2+}, while not affecting V_{max} of the enzyme, decreased the binding affinity of NAD^+ to apo-SAHH. This was further evidenced by release of the NAD^+ cofactor upon Cu^{2+} binding. Gomi et al. (*32*) revealed that SAHH bound tightly one NAD^+ cofactor at each subunit with a K_d of $\sim$100 nM; however, upon Cu^{2+} binding, the NAD^+ binding affinity was reduced greatly (Figure 3). Since the substrate-free NAD^+-form enzyme was in the open conformation proposed by Yin et al. (*8*), NAD^+ was readily released upon binding of Cu^{2+} in a concentration-dependent manner (Figure 2). Because release of the NADH cofactor from the substrate-bound NADH-form enzyme was not observed, copper ions did not eliminate the partial redox reaction between the enzyme-bound NAD^+ and substrates. Therefore, release of the NAD^+ cofactor should account for loss of the partial redox activity and ultimately the total loss of activity. Also, it is possible that the substrate binds to the Cu^{2+}-bound holoenzyme, and the catalytic reaction is stopped after the first oxidation of substrate (i.e., the bound NAD^+ is reduced to NADH).

The proposed mechanism was in agreement with our previous studies (*28*) that the substrate Ado decreased the inhibitory potency of Cu^{2+}. In the presence of Ado, SAHH would exist primarily as ENADH (K_{Ado}), due to the reduction of NAD^+ by Ado. Since the equilibrium constant (K_2) was

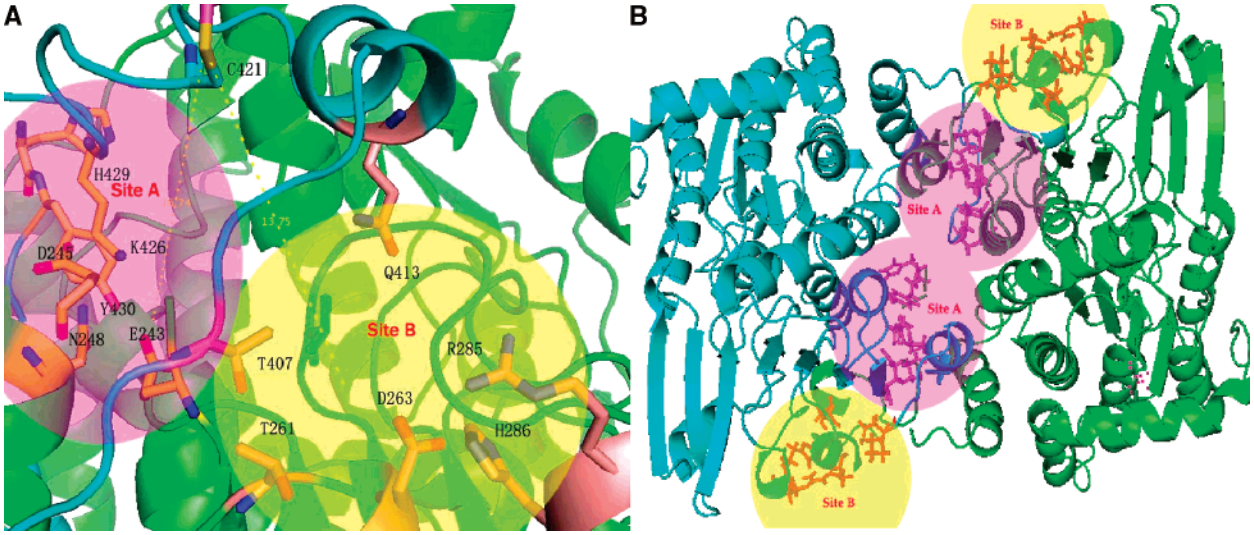

FIGURE 6: Tentative Cu^{2+} binding sites on SAHH suggested by computational simulation: (A) side view; (B) top view. The sulfide atom of Cys421 is bright orange in color, and the proposed residues possibly in coordination with Cu^{2+} are salmon in color. Subunits A and B of SAHH are green and cyan in color, respectively. Computational searches for proton acceptors were done on crystal structure 1A7A using an Insight II program. The distance between the centers of site A (or B) within one dimer is 10 Å (or 40 Å). See the text for details.

Scheme 1

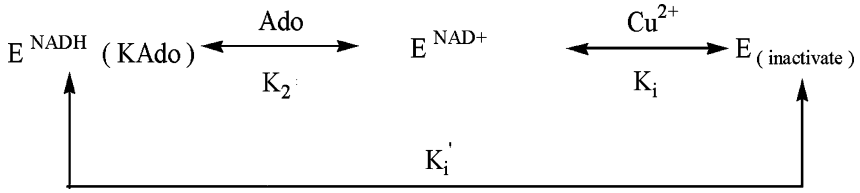

determined previously by Porter et al. (*18*) to be 7.5, the apparent inhibition constant in the presence of Ado would be $K_i' = K_2K_i = 25 \times 7.5 \approx 180$ nM, which is almost identical to our previously estimated value (160 ± 10 nM) (*28*).

Copper Ion Binding Sites on SAHH. On the basis of the protein structure and the effect of Ado on the potency of Cu^{2+}, we previously proposed that Cu^{2+} might bind to a position near the active sites (*28*); however, the inhibition mechanism described above has ruled out this possibility. The inhibition kinetics suggested that Cu^{2+} could bind to the cofactor binding domain of the enzyme, since Cu^{2+} does not bind at the substrate sites and binding of NAD^+ cofactor was greatly affected.

Studies by circular dichroism (CD) spectroscopy and limited proteolysis suggested that the specific binding of Cu^{2+} did not result in significant changes in secondary or tertiary structures of SAHH (data not shown). As the crystallization of Cu−SAHH complexes has not been successful, ESR was used to determine the location of Cu^{2+}. The specifically bound Cu^{2+} exhibited a very weak ESR signal (Figure 6), suggesting that the Cu^{2+} binding sites on SAHH must be very close to each other. In the tetrameric enzyme, Hu et al. (*15*) proposed that there is a unique channel structure (~10 × 10 × 50 Å) in the central core composed of four sets of three helices (181−257, 421−432), and metal ions might bind inside the channel and regulate the function of SAHH (*15*). Cu^{2+} sites inside the channel would explain the absence of a Cu^{2+} signal in ESR studies.

Since the ESR signal was too weak to provide useful information for Cu^{2+} coordination, Cys421 of SAHH was labeled with a maleimide spin probe to further investigate the location of Cu^{2+} sites. Cys421 was at the C-terminal domain of SAHH, which covered the entrance of the central channel. The interaction of the spin label with enzyme-bound Cu^{2+} provided distance information between Cu^{2+} and the free radical of the spin label. Cu^{2+} significantly reduced the ESR signal of the spin probe, Figure 5. The distance between the free radical of the probe and Cu^{2+} was calculated to be 8.6 Å. Within this distance, two possible copper binding sites were identified, Figure 6. Site A was located within the central channel, surrounded by proton acceptors of Glu243, Asp 245, Asn248, Lys426, His429, and Tyr430. It is possible that Cu^{2+} might bind at site A with four of the above amino acid residues. Site B was outside the channel, so it can be excluded from the specific Cu^{2+} site because the distance (~40 Å) between B sites was too far to support strong spin−spin interactions.

On the basis of the structure of this tentative Cu^{2+} binding site, the effect of Cu^{2+} on dissociation of the NAD^+ cofactor could be explained. Previous studies of SAHH mutation on Lys426 (*40*) or Asp245 (Asp244 in rat enzyme) (*1*) or certain other residues in the C-terminal domain (*41*, *42*) would result in inactive mutant enzymes. The NADH cofactor was trapped in the closed conformation of enzyme, but NAD^+ cofactor would be released. The crystal structure of a D244E mutant of rat SAHH suggested that the residues Lys425, His428, and Tyr429 of one subunit form a complex hydrogen bond network with the cofactor NAD^+. Asn247, Asp244, and Asp181 in the other subunit of the dimerized enzyme form a tetrameric enzyme with two dimers. As described above, these residues (corresponding to the residues D245, Lys426, His429, Tyr430, Asn248, Asp245, and Asp182 in human enzyme, respectively) were involved in Cu^{2+} binding. Since

this hydrogen bond network was crucial for NAD^+ binding, Cu^{2+} binding could definitely interrupt the network and cause dissociation of the NAD^+ cofactor. The effect of copper ions in releasing the NAD^+ cofactor but trapping of NADH in the closed conformation resembled that of the mutants previously described.

A Clue for the Physiological Function of Cu^{2+}−SAHH Interaction. The apparent inhibition constant of Cu^{2+} on the SAHH activity was determined to be ~25 nM. In cytoplasm, the presence of Ado will increase this value by the mechanism described above. Then the effective concentration of Cu^{2+} on the activity of SAHH would be close to the binding affinity of the NAD^+ cofactor to SAHH; thus, Cu^{2+} may work with NAD^+ in regulating the intracellular SAHH activity. This postulation might be helpful in understanding the antiviral, antiarthritic, and other biological activities of copper compounds. The regulation of SAHH activity by Cu^{2+} and NAD^+ suggests that SAHH could provide a link coupling biomethylation processes and the redox states of cells.

In conclusion, the mechanism by which Cu^{2+} ions inhibit the activity of SAHH was investigated. Cu^{2+} may bind to the central channel of SAHH and interrupt the hydrogen bond network between the cofactor NAD^+ and enzyme subunits, causing the release of the NAD^+ cofactor. The action of copper ions on SAHH may be helpful in understanding the biological effects of copper compounds.

ACKNOWLEDGMENT

We thank Prof. John J. Hefferren for editing the manuscript.

REFERENCES

1. Komoto, J., Huang, Y., Gomi, T., Ogawa, H., Takata, Y., Fujioka, M., and Takusagawa, F. (2000) Effects of site-directed mutagenesis on structure and function of recombinant rat liver S-adenosylhomocysteine hydrolase. Crystal structure of D244E mutant enzyme, *J. Biol. Chem. 275*, 32147−32156.
2. Backlund, P. S., Carotti, D., and Cantoni, G. L. (1986) Effects of the S-adenosylhomocysteine hydrolase inhibitors 3-deazaadenosine and 3-deazaaristeromycin on RNA methylation and synthesis, *Eur. J. Biochem. 160*, 245−251.
3. Refsum, H., Ueland, P. M., Nygard, O., and Vollset, S. E. (1998) Homocysteine and cardiovascular disease, *Annu. Rev. Med. 49*, 31−62.
4. de Luis, D. A., Fernandez, N., Arranz, M. L., Aller, R., Izaola, O., and Romero, E. (2005) Total homocysteine levels relation with chronic complications of diabetes, body composition, and other cardiovascular risk factors in a population of patients with diabetes mellitus type 2, *J. Diabetes Complications 19*, 42−46.
5. Poirier, L. A., Wise, C. K., Delongchamp, R. R., and Sinha, R. (2001) Blood determinations of S-adenosylmethionine, S-adenosylhomocysteine, and homocysteine: correlations with diet, *Cancer Epidemiol., Biomarkers Prev. 10*, 649−655.
6. Clarke, R., Smith, A. D., Jobst, K. A., Refsum, H., Sutton, L., and Ueland, P. M. (1998) Folate, vitamin B12, and serum total homocysteine levels in confirmed Alzheimer disease, *Arch. Neurol. 55*, 1449−1455.
7. Nilsson, K., Gustafson, L., and Hultberg, B. (2002) Role of impaired renal function as a cause of elevated plasma homocysteine concentration in psychogeriatric patients, *Scand. J. Clin Lab. Invest. 62*, 385−389.
8. Yin, D., Yang, X., Hu, Y., Kuczera, K., Schowen, R. L., Borchardt, R. T., and Squier, T. C. (2000) Substrate binding stabilizes S-adenosylhomocysteine hydrolase in a closed conformation, *Biochemistry 39*, 9811−9818.
9. Turner, M. A., Yang, X., Yin, D., Kuczera, K., Borchardt, R. T., and Howell, P. L. (2000) Structure and function of S-adenosylhomocysteine hydrolase, *Cell Biochem. Biophys. 33*, 101−125.
10. Bohlin, A. B., and Berg, U. (1991) Renal functional adaptation of the adult kidney following transplantation to the child, *Kidney Int. 39*, 129−134.
11. Kroll, K., Decking, U. K., Dreikorn, K., and Schrader, J. (1993) Rapid turnover of the AMP-adenosine metabolic cycle in the guinea pig heart, *Circ. Res. 73*, 846−856.
12. Fredholm, B. B., and Hedqvist, P. (1980) Modulation of neurotransmission by purine nucleotides and nucleosides, *Biochem. Pharmacol. 29*, 1635−1643.
13. Chiang, P. K. (1998) Biological effects of inhibitors of S-adenosylhomocysteine hydrolase, *Pharmacol. Ther. 77*, 115−134.
14. Yang, X., Hu, Y., Yin, D. H., Turner, M. A., Wang, M., Borchardt, R. T., Howell, P. L., Kuczera, K., and Schowen, R. L. (2003) Catalytic strategy of S-adenosyl-L-homocysteine hydrolase: transition-state stabilization and the avoidance of abortive reactions, *Biochemistry 42*, 1900−1909.
15. Hu, Y., Komoto, J., Huang, Y., Gomi, T., Ogawa, H., Takata, Y., Fujioka, M., and Takusagawa, F. (1999) Crystal structure of S-adenosylhomocysteine hydrolase from rat liver, *Biochemistry 38*, 8323−8333.
16. Turner, M. A., Yuan, C. S., Borchardt, R. T., Hershfield, M. S., Smith, G. D., and Howell, P. L. (1998) Structure determination of selenomethionyl S-adenosylhomocysteine hydrolase using data at a single wavelength, *Nat. Struct. Biol. 5*, 369−376.
17. Porter, D. J. (1993) S-adenosylhomocysteine hydrolase. Stereochemistry and kinetics of hydrogen transfer, *J. Biol. Chem. 268*, 66−73.
18. Porter, D. J., and Boyd, F. L. (1992) Reduced S-adenosylhomocysteine hydrolase. Kinetics and thermodynamics for binding of 3′-ketoadenosine, adenosine, and adenine, *J. Biol. Chem. 267*, 3205−3213.
19. Porter, D. J., and Boyd, F. L. (1991) Mechanism of bovine liver S-adenosylhomocysteine hydrolase. Steady-state and pre-steady-state kinetic analysis, *J. Biol. Chem. 266*, 21616−21625.
20. Abeles, R. H., Tashjian, A. H., Jr., and Fish, S. (1980) The mechanism of inactivation of S-adenosylhomocysteinase by 2′-deoxyadenosine, *Biochem. Biophys. Res. Commun. 95*, 612−617.
21. Palmer, J. L., and Abeles, R. H. (1979) The mechanism of action of S-adenosylhomocysteinase, *J. Biol. Chem. 254*, 1217−1226.
22. Yamada, T., Takata, Y., Komoto, J., Gomi, T., Ogawa, H., Fujioka, M., and Takusagawa, F. (2005) Catalytic mechanism of S-adenosylhomocysteine hydrolase: roles of His 54, Asp130, Glu155, Lys185, and Aspl89, *Int. J. Biochem. Cell Biol. 37*, 2417−2435.
23. Bethin, K. E., Petrovic, N., and Ettinger, M. J. (1995) Identification of a major hepatic copper binding protein as S-adenosylhomocysteine hydrolase, *J. Biol. Chem. 270*, 20698−20702.
24. Petrovic, N., Comi, A., and Ettinger, M. J. (1996) Copper Incorporation into Superoxide Dismutase in Menkes Lymphoblasts, *J. Biol. Chem. 271*, 28335−28340.
25. Mansoor, M. A., Bergmark, C., Haswell, S. J., Savage, I. F., Evans, P. H., Berge, R. K., Svardal, A. M., and Kristensen, O. (2000) Correlation between plasma total homocysteine and copper in patients with peripheral vascular disease, *Clin. Chem. 46*, 385−391.
26. Hultberg, B., Andersson, A., and Isaksson, A. (1997) Copper ions differ from other thiol reactive metal ions in their effects on the concentration and redox status of thiols in HeLa cell cultures, *Toxicology 117*, 89−97.
27. McArdle, H., Bingham, M., Summer, K., and Ong, T. (1999) Cu metabolism in the liver, *Adv. Exp. Med. Biol. 448*, 29−37.
28. Chen, J., and Liu, Q. (2002) Copper ions' inhibition on activity of S-AdenosylHomocysteine hydrolase, *Chin. Sci. Bull. 47*, 421−424.
29. Li, Y., Chen, J., Liu, J., Yang, X., and Wang, K. (2004) Binding of Cu2+ to S-adenosyl-L-homocysteine hydrolase, *J. Inorg. Biochem. 98*, 977−983.
30. Yuan, C. S., Ault-Riche, D. B., and Borchardt, R. T. (1996) Chemical modification and site-directed mutagenesis of cysteine residues in human placental S-adenosylhomocysteine hydrolase, *J. Biol. Chem. 271*, 28009−28016.
31. Bradford, M. M. (1976) A rapid and sensitive method for the quantitation of microgram quantities of protein utilizing the principle of protein-dye binding, *Anal. Biochem. 72*, 248−254.
32. Gomi, T., Takata, Y., and Fujioka, M. (1989) Rat liver S-adenosylhomocysteinase. Spectrophotometric study of coenzyme binding, *Biochim. Biophys. Acta 994*, 172−179.
33. Yuan, C. S., Liu, S., Wnuk, S. F., Robins, M. J., and Borchardt, R. T. (1994) Mechanism of inactivation of S-adenosylhomocys-

teine hydrolase by (E)-5′,6′-didehydro-6′-deoxy-6′-halohomoadenosines, *Biochemistry 33*, 3758−3765.
34. Pali, T., Finbow, M. E., and Marsh, D. (2006) A divalent-ion binding site on the 16-KDa proton channel from Nephrops norvegicus-revealed by EPR spectroscopy, *Biochim. Biophys. Acta 1758*, 206−212.
35. Cohn, M., Diefenbach, H., and Taylor, J. S. (1971) Magnetic resonance studies of the interaction of spin-labeled creatine kinase with paramagnetic manganese-substrate complexes, *J. Biol. Chem. 246*, 6037−6042.
36. Yang, X., and Borchardt, R. T. (2000) Overexpression, purification, and characterization of S-adenosylhomocysteine hydrolase from Leishmania donovani, *Arch. Biochem. Biophys. 383*, 272−280.
37. Fujioka, M., and Takata, Y. (1981) S-Adenosylhomocysteine hydrolase from rat liver. Purification and some properties, *J. Biol. Chem. 256*, 1631−1635.
38. Bethin, K. E., Cimato, T. R., and Ettinger, M. J. (1995) Copper binding to mouse liver S-adenosylhomocysteine hydrolase and the effects of copper on its levels, *J. Biol. Chem. 270*, 20703−20711.
39. Taylor, J. S., Leigh, J. S., Jr., and Cohn, M. (1969) Magnetic resonance studies of spin-labeled creatine kinase system and interaction of two paramagnetic probes, *Proc. Natl. Acad. Sci. U.S.A. 64*, 219−226.
40. Ault-Riche, D. B., Yuan, C. S., and Borchardt, R. T. (1994) a single mutation at lysine 426 of human placental s-adenosylhomocysteine hydrolase inactivates the enzyme, *J. Biol. Chem. 269*, 31472−31478.
41. Porcelli, M., Cacciapuoti, G., Fusco, S., Iacomino, G., Gambacorta, A., De Rosa, M., and Zappia, V. (1993) S-adenosylhomocysteine hydrolase from the thermophilic archaeon Sulfolobus solfataricus: purification, physico-chemical and immunological properties, *Biochim. Biophys. Acta 1164*, 179−188.
42. Porcelli, M., Cacciapuoti, G., Fusco, S., Bertoldo, C., De Rosa, M., and Zappia, V. (1996) Cloning and sequencing of the gene coding for S-adenosylhomocysteine hydrolase in the thermophilic archaeon Sulfolobus solfataricus, *Gene 177*, 17−22.

BI700395D